

# HIGH PERFORMANCE SHORT-PERIOD UNDULATORS USING HIGH TEMPERATURE SUPERCONDUCTOR TAPES\*

S. Prestemon, D. Dietderich, A. Madur, S. Marks, R.D. Schlueter,  
Lawrence Berkeley National Laboratory, Berkeley, Ca. USA

## Abstract

Superconducting undulators are currently under development at a number of light sources to serve as the next generation of insertion devices, with higher fields providing enhanced spectral range for users. Most of these devices are designed with wire-based technologies appropriate for periods greater than 10mm. New undulator concepts yielding very short-period, high-field devices with periods of a few millimeters and a  $K \sim 1$  have the potential to significantly reduce the cost and enhance the performance of FEL's. Here we describe a design using high temperature superconductor tapes that are commercially available, and that promise a cost-effective fabrication process using micromachining or lithography.

## INTRODUCTION

The synchronicity condition for synchrotron radiation relates the emitted electromagnetic radiation wavelength  $\lambda_1$  to the electron energy  $E$  and the undulator spatial period  $\lambda_u$ . For planar undulators the condition is

$$\lambda_1 = \frac{1 + K^2/2}{\gamma^2} \lambda_u; \quad K = \frac{eB_0\lambda_u}{2\pi mc} \quad (1)$$

where  $\gamma = E/E_0$  is the (electron) relativistic mass ratio; the deflection parameter  $K$  is defined with  $B_0$  the undulator maximum on-axis field,  $m$  the electron rest mass, and  $c$  the speed of light. The photon production is a strong function of the deflection parameter, peaking around  $K = 1$ . To provide users with variable radiation wavelength the FEL can be designed to scan by varying electron energy or by modulating the field strength.

Undulator technology is characterized by performance curves describing  $B_0(\lambda_u, g_v)$ , where  $g_v$  is the vacuum aperture of the FEL. Recent concepts in X-ray FEL design motivate the development of very short period undulators, with the promise of dramatically shorter and more cost-effective FEL lines. Here we describe an undulator concept that is ideally suited to an operating regime  $g_v \sim 2$ mm and  $5 < \lambda_u < 10$ mm, of significant interest to the X-ray FEL community.

\* This work is supported by the Director, Office of Science, U. S. Department of Energy under Contract No. DE-AC02-05CH11231.

## HIGH TEMPERATURE SUPERCONDUCTOR TAPE

The high-temperature superconductor YBCO ( $\text{YBa}_2\text{Cu}_3\text{O}_7$ ) has a transition temperature of 120K and critical fields in excess of 100T. Very high transport current can be maintained in the material, provided it is in single-crystal form; grain boundaries hinder current transport in polycrystalline material unless the grain orientation is strictly controlled. The material is therefore typically fabricated by growing YBCO on a substrate that has been appropriately prepared, for example with buffer layers for precise texture on which crystal growth can occur. The final material is in the form of a tape of width  $w$  and total thickness  $t$  (see Fig. 1).

Since the texture emanates from the buffer layer, the quality of grain alignment decreases with YBCO thickness. Commercially available tapes are usually limited to  $1 - 2\mu\text{m}$  of YBCO. The material is highly strain sensitive; to provide tape flexibility the conductor is structured with the YBCO layer near the center. Note the Cu stabilizer surrounding the conductor, of importance for current stability and magnet protection for applications involving significant stored energy, e.g. high-field solenoids and accelerator magnets. The Nickel-alloy substrate provides mechanical support, again of importance for traditional magnet applications.

The critical transport current  $J_{sc}$  in the YBCO layer is a function of temperature, applied magnetic field, and strain. A typical value in commercial tapes is  $J_{sc}(77\text{K}, 0\text{T}) \sim 30\text{kA}/\text{mm}^2$ ; at 4.2K the value increases by a factor  $> 12$ . These current densities are dramatically higher ( $\sim 10$ ) than can be obtained with conventional low-temperature superconductors (LTS) (see [1] for a comparison of superconductor performance). LTS benefit, however, from higher average current densities: the area ratio of superconductor to normal metal in the YBCO tapes is  $\sim 1 - 3\%$  as compared to 25 - 50% for LTS materials.

## TAPE UNDULATOR CONCEPT

Traditional superconducting undulator concepts use layered windings on a machined former to generate the alternating fields. This approach is not readily applied with tape conductors, as some degree of "hard-way" bend of the tape is usually required, or a large number of joints must be made. Here we propose to eliminate the need for windings altogether by incorporating the current path directly onto the tape. Using micromachining or lithography techniques,

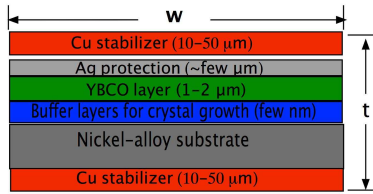


Figure 1: Example of  $\text{YBa}_2\text{Cu}_3\text{O}_7$  conductor architecture. The Hastelloy substrate provides mechanical strength; Cu stabilizer provides current stability and protection in the event of a quench. Multiple buffer layers are used to create appropriate texture for proper YBCO crystal growth.

a flat YBCO tape conductor can be machined with grooves that force the current in a defined path, as shown in Fig. 2. The YBCO tape properties can be leveraged by close proximity of the YBCO layer to the beam, resulting in efficient use of field-producing current.

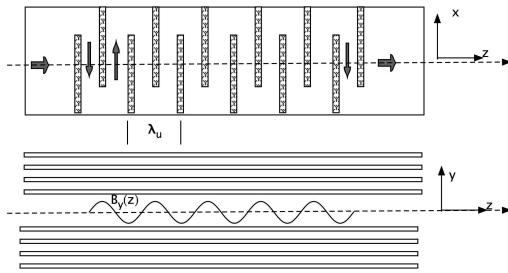


Figure 2: Basic concept of the tape undulator (top). Transport current flows from left to right; the vertical cuts dictate an oscillating current path. Multiple layers can be superimposed to yield additional field strength. The resulting alternating current direction creates a field  $B_y(z) \sim B_0 \text{Sin}(2\pi z/\lambda_u)$  as seen by the passing electron (bottom). The dotted line represents the general electron trajectory.

A series of alternating line current pairs located symmetrically about the real axis ( $\text{Im}(z) = \pm a$ ) generate an on-axis field

$$B_y(z) = \frac{\mu_0 I}{2\pi} \text{Re} \left[ \sum_k k (-1)^k \left( \frac{1}{z - z_k} + \frac{1}{z - z_k^*} \right) \right] \quad (2)$$

The resulting field profile is shown in Fig 3.

The line current model (Eq. 2) can be replaced by a more accurate current sheet model by integrating a current density  $\tilde{J}[A/m]$  a distance  $\delta < \lambda_u/2$  beyond each source location  $z_k = x_k \pm ia$ , yielding (for  $z$  on the real axis)

$$B_y(z) = \frac{\mu_0 \tilde{J}}{\pi} \text{Re} \left[ \sum_k (-1)^k \ln \frac{a^2 + (\delta + x_k - z)^2}{a^2 + (x_k - z)^2} \right] \quad (3)$$

The finite length of a line (or sheet) current impacts the field produced. Let  $\xi = L/(2\Delta z)$ , where  $\Delta z$  is the distance from the beam location to the line current, and  $L$  is the length of the current path transverse to the beam. The

## Light Sources and FELs

### T15 - Undulators and Wigglers

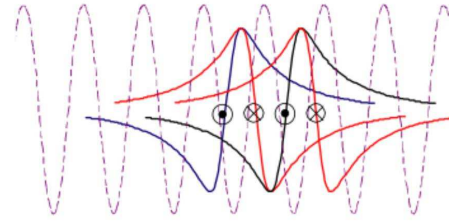


Figure 3: Plot of the fields generated by alternating line currents. The line currents are perpendicular to the page; the blue (positive current) and red (negative current) lines represent  $B_y(z)$  fields generated by the corresponding line current. A series of alternating line currents generates the oscillatory field (dotted line).

field amplitude  $\|B\|$  is then reduced by the fraction

$$\frac{\|B\|}{\|B_{inf}\|} = \frac{\xi}{\sqrt{1 + \xi^2}} \quad (4)$$

where  $B_{inf}$  is the field produced by infinite line currents. The line currents should therefore have a length  $L > \lambda$  to yield performance  $\|B\|/\|B_{inf}\| > 90\%$ . Commercially available tapes are manufactured in widths of many *cm*'s. Note that current transitions at the edges will also generate (presumably unwanted) multipole fields that are also minimized by longer current path lengths  $L$ .

A number of current sheets, i.e. tapes, can be superimposed via stacking. The current is passed in series from one stack to another, with the line pattern (Fig. 2) shifted by one line from layer to layer to yield superimposed line currents of appropriate direction as the current flows back and forth. The edge currents of consecutive layers yield compensating multipole terms, significantly reducing their effects.

## PERFORMANCE CHARACTERISTICS

Performance of undulators is characterized by the function  $B(g_v, \lambda_u)$ , where  $g_v$  is the beam vacuum aperture. Here we provide a comparison with existing competing technologies: permanent magnet in-vacuum undulators (IVID) and superconducting helical undulators using low-temperature superconductors.

### Permanent Magnet In-vacuum Devices

IVID devices are typically constructed using the "hybrid" approach, wherein permanent magnet (PM) material is used to place magnetic steel poles on a scalar potential [2], as apposed to pure permanent magnet devices that rely solely on the PM flux. Both types have performance characterized by the function

$$B(g_v, \lambda_u) = a B_r e^{-b(g/\lambda_u) + c(g/\lambda_u)^2} \quad (5)$$

where  $B_r$  is the remanent field of the permanent magnet material and the coefficients  $a$ ,  $b$ , and  $c$  are provided in Table 1.

Table 1: PM Based Undulator Fit Coefficients (see Eq. 5)

Type	a	b	c
Pure permanent magnet	1.72	$\pi$	0
Hybrid permanent magnet	3.13	5.08	1.54

### Superconducting Helical Undulators

Bifilar helical undulators using low-temperature superconducting wires have been used since the 1970's [3]. The on-axis field [4] of a bifilar helical line current of radius  $r$  can be integrated over a realistic cross-section of dimension  $(r_0, r_1) \times \lambda_u/2$  to yield

$$\|B\| = \frac{\alpha r_0}{\sqrt{r_0^2 + \lambda_u^2/4\pi^2}} \frac{2\mu_0 J_E}{\pi^2} [\lambda_u F_1 + \pi F_2] \quad (6)$$

with

$$F_1 = K_0\left(\frac{2\pi r_0}{\lambda_u}\right) - K_0\left(\frac{2\pi r_1}{\lambda_u}\right)$$

$$F_2 = 2r_0 K_1\left(\frac{2\pi r_0}{\lambda_u}\right) - 2r_1 K_1\left(\frac{2\pi r_1}{\lambda_u}\right).$$

Here  $K_0$  and  $K_1$  are modified Bessel functions. The coefficient  $\alpha$  has been added to account for a realistic winding former; assuming a former coilpack separation of  $\delta z = \lambda_u/5$  results in  $\alpha \approx 0.8$ . The variation in pitch angle with radius is not accounted for in Eq. 6, although the effect is small, typically 1 – 5%.

### Performance Comparison

The fact that Eq. 5 is homogeneous, whereas Eq. 3 and 6 are not, suggests that different technologies excel in different regimes of  $\lambda_u$  and  $g_v$ . A comparison is provided in Fig. 4 for the important regime  $5 < \lambda_u < 10mm$ , for a beam aperture of  $\sim 2mm$ . Permanent magnets are competitive at fairly large  $g_v/\lambda_u$  ratio's, although the HTS tape concept excels throughout this period range. The helical SCU data falls short of the HTS concept due to the larger magnetic gap of  $3mm$ , needed to allow for a winding mandrel/vacuum chamber. For some FEL applications, however, the helical SCU is preferred due to the continuous acceleration it provides, resulting in higher photon flux.

The PM in-vacuum data suggests strong performance at short periods. Although devices with periods of  $10mm$  or less have been built, their fabrication requires precise machining of magnetic material and of poles, followed by labor-intensive assembly and shimming. These issues become more severe as the period and gap decrease. Strengths of the HTS concept are that a) periodicity can be accurately maintained using existing micromachining capabilities, b) the assembly is fairly simple, and c) the device cost is therefore expected to be low. These issues are particularly important for large-scale FEL applications that may require 10 – 100m of undulators.

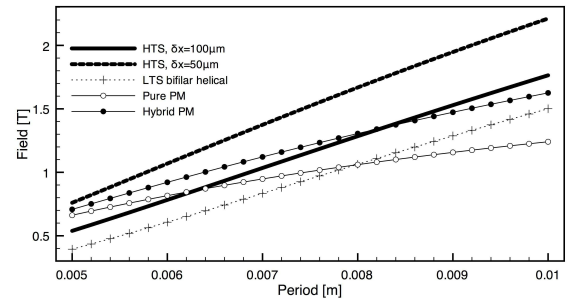


Figure 4: Performance comparison between PM, PM-hybrid, superconducting bi-filar helical, and the proposed HTS tape concept technologies. A stack of 25 tapes was assumed for the calculations.  $100\mu m$  tape is a standard commercial product;  $50\mu m$  tape can be readily obtained by eliminating the stabilizer material. Calculations for superconducting technologies neglect  $J_c(B)$ , and are only valid for  $B < 2T$ . The bifilar helical SCU data assumes  $J_E = 2000A/mm^2$ , but does not consider the possible use of iron between coils. PM-based devices assume remanence field  $Br = 1.35T$ .

### CONCLUDING REMARKS

The proposed HTS tape undulator concept shows potential to excel for short-period FEL applications. A number of issues need to be addressed: a) demonstrate that the anticipated transport current can be maintained, b) demonstrate that the current distribution in each sheet is sufficiently reproducible, c) evaluate the influence of image currents on the superconductor.

It should be noted that this concept can be extended to very short period devices, e.g. sub-mm with beam apertures of a few hundred microns while maintaining  $K \sim 1$ , for future "table-top FEL" applications. Accurate control of the period under such conditions can be provided using lithography techniques during the YBCO-layer deposition. The proposed stacked-layer approach also provides the possibility of introducing focussing through appropriate current path definitions on one or more dedicated layers.

### REFERENCES

- [1] Peter Lee, <http://www.magnet.fsu.edu/magnettechnology/research/asc/plots.html>.
- [2] R.D. Schlueter, in "Synchrotron Radiation Sources: a Primer", Ed. H. Winick, World Scientific, 1994.
- [3] L.R. Elias, J. M. Madey, "Superconducting helically wound magnet for the free-electron laser", Review of Scientific Instrumentation, 1979 vol. 50 (11) pp. 6
- [4] B. Kincaid, "A short-period helical wiggler as an improved source of synchrotron radiation", Journal of Applied Physics, 1977